Array of time-of-flight diamond detectors for particle discrimination in laser driven p-^{11}B fusion experiments

Published by IOP Publishing for Sissa Medialab
Received: *May 10, 2023*
Accepted: *June 13, 2023*
Published: *July 7, 2023*

2nd International Workshop on Proton-Boron Fusion
Catania, Italy
5–8 September 2022

Array of time-of-flight diamond detectors for particle discrimination in laser driven p-^{11}B fusion experiments

C. Verona,[a,*] **M. Marinelli,**[a] **A.M. Raso,**[a] **G. Verona Rinati,**[a] **G.A.P. Cirrone,**[b,c] **G. Petringa,**[b] **L. Giuffrida,**[b,d] **J. Dostál,**[e,f] **M. Krupka**[e,f] **and F. Consoli**[g]

[a] *Dipartimento Ing. Industriale, Università di Roma "Tor Vergata", Via del Politecnico 1, Roma 00133, Italy*
[b] *Laboratori Nazionali del Sud, INFN, Via S. Sofia 62, Catania 95125, Italy*
[c] *CSFNSM — Centro Siciliano Fisica Nucleare e Struttura della Materia, Via S. Sofia 64, Catania 95123, Italy*
[d] *ELI Beamlines Facility, The Extreme Light Infrastructure ERIC, Za Radnicí 835, 252 41 Dolni Brezany, Czech Republic*
[e] *Laser Plasma Department, Institute of Plasma Physics, Za Slovankou 3, 182 00 Prague 8, Czech Republic*
[f] *Department of Radiation and Chemical Physics, Institute of Physics, Na Slovance 2, 182 00 Prague 8, Czech Republic*
[g] *ENEA, Fusion and Security Department, C.R. Frascati, Via Enrico Fermi 45, Frascati 00044, Italy*

E-mail: claudio.verona@uniroma2.it

Abstract: The detection of radiation emission in laser induced plasma experiments is an helpful method for gaining information on the physics of laser-matter interaction. Time-of-Flight (TOF) approach is a powerful and effective method to obtain timely spectra of particles accelerated from laser-generated plasma. To this respect, diamond-based detectors are very attractive due to their interesting features such as fast signal collection time, signal proportional to the energy deposited by the incident radiation, blindness to visible radiation, high radiation hardness and low leakage current at room temperature operation. Unfortunately, they cannot supply discrimination on the species of the incoming ions, but only their energies. This may be overcome using specific filtering foils to exploit the different stopping powers of ions of different species and energies. In this work we describe the method to distinguish particles using an array of TOF diamond detectors. A first prototype array, consisting of 2×2 diamond detectors, nominally identical and featuring by aluminum filters of different thicknesses, was developed and preliminary tested at PALS facility in Prague.

Keywords: Diamond Detectors; Instrumentation and methods for time-of-flight (TOF) spectroscopy; Radiation-hard detectors

*Corresponding author.

https://doi.org/10.1088/1748-0221/18/07/C07008

2023 JINST 18 C07008

Contents

2023 JINST 18 C07008

1 Introduction

Thanks to the development of new and powerful lasers, in recent decades the technology of particle acceleration using plasma generated by powerful lasers has made great progress [1, 2]. The interest in this field comes from the possibility of generating, with a compact system, intense high-energy bunches of particles that can be used for several applications such as diagnostics for cultural heritage [3], radiobiology [4] and inertial confinement fusion [5]. The nuclear reaction between protons and boron ions is one of the most promising in nuclear fusion research. This reaction has been deeply studied [6–8] during the past decades. It uses the ^{11}B isotope and a proton as the catalyst for the fusion reaction, resulting in the production of three α-particles with a highly peaked energy spectrum at ~4 MeV, spanning a wide energy range (up to 7 MeV in the laboratory reference system) [9, 10]. The high interest in this type of nuclear fusion reaction (from now on p-^{11}B) lies on its property of being essentially aneutronic and on the use of non-radioactive reagents, which are also abundant in nature. Moreover, the p-^{11}B reaction has also useful implications in multiple applications. In the medical field for example, with the so-called Proton-Boron Capture Therapy (PBCT), approach where this reaction could improve the radiobiology effectiveness of a standard protontherapy treatment [11–13]. Studies have shown potential application of the α generated by the reaction as medical radioisotopes for therapy, imaging and diagnostic purposes [14, 15]. Still, the gamma rays emitted in the reaction can be exploited for online imaging and dose monitoring during cancer treatment [16, 17]. In the last 15 years, p-^{11}B fusion has been effectively induced by means of high-power lasers, reporting an impressive progression in the reaction yield [10, 18–20]. Several experiments were carried out using the kJ-class, sub-ns PALS [18, 20] laser with hydrogenated boron targets obtaining highest α-particle flux to date, i.e. above 10^{10}/sr/pulse. In the experimental study of the p-^{11}B fusion reaction, one of the critical experimental issue is the definition of a trustable detector allowing to discriminate alpha particles from the other charged particles produced from the laser plasma interaction [21]. Single-crystal diamond detectors are widely employed for the ion diagnostic in laser-generated plasma experiments. In particular, diamonds are used as Time-of-Flight

(TOF) detectors characterized by good sensitivity, high radiation hardness and fast time response, being blindness to visible radiation and having low leakage current at room temperature [22, 23]. The TOF technique makes it possible to derive the kinetic energies of accelerated particles by measuring the time the particles take to cover the distance between the point of generation and the detector. Nevertheless, the TOF technique, without any arrangements, is not capable to discriminate alpha particles generated from p-^{11}B fusion reaction from the laser-driven protons and ions. To this respect, recent studies [24] have shown that solid- state nuclear track detectors, CR-39 type, coupled with Thomson Parabola spectrometer prove possible to discriminate α particles from protons and ions generated in the p-^{11}B fusion reaction. However, this is an off-line and time-consuming method. In this work we present the design and implementation of a first prototype of an array diamond detector. A relatively new and simple method for discriminating particle species consisting of the combined use of obscured diamond detectors with material layers and TOF technique is described. Such device was preliminary tested at PALS facility in Prague, using hydrogenated silicon targets.

2 Materials and methods

2.1 Diamond detector array prototype

The prototype consists of an array of 2×2 diamond-based detectors named D_{11}, D_{12}, D_{21} and D_{22} (figure 1c), all operating in planar configuration [25]. Each detector was fabricated at Industrial Engineering Department laboratories of "Tor Vergata" University as described below. About 30 µm thick high-quality diamond layer was deposited by Microwave Plasma Enhanced Chemical Vapor Deposition (MWPECVD) on a commercial low-cost synthetic diamond substrate, 3×3×0.3 mm^3 in size. The thickness of diamond detectors allows normally-incident protons up to 2.2 MeV and He ions up to 9 MeV to fully stop within its sensitive volume. The diamond film was cleaned and thermal annealed at 500°C in air to remove hydrogen bond on the surface. Interdigitated chromium electrodes were then realized by photolithography techniques and thermal evaporation of chromium on diamond surface. The width and distance between the electrodes are 20 µm as shown in figure 1a. The active area of detectors is about 1 mm^2. The diamond detectors were wire bonded on a dedicated PCB for electrical connections equipped with four integrated bias tees (R = 1 MΩ and C = 1 µF) for biasing each detector (figure 1b). They were then arranged in a 2×2 array at 3 cm apart. The PCB was mounted inside an aluminum holder featured by SMA connectors: 4 for output signals and 1 for the bias (figure 1c). An external voltage of 60 V was applied for all detectors. The detector outputs were connected to a fast oscilloscope (4 channels) by low noise coaxial cables. The time resolution of each diamond detector is less of 1 ns, as obtained from detection of single 5.5 MeV α particle emitted by ^{241}Am source [26]. Aluminum layers of different thicknesses were placed in front of three diamond detectors to provide different energy cut-off for different particles, thus to allow particle species identification.

2023 JINST 18 C07008

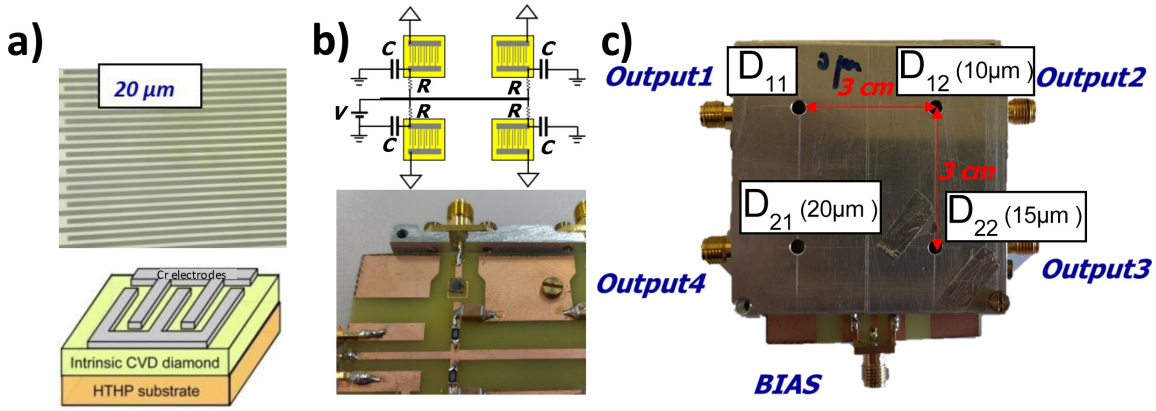

Figure 1. Depiction of the interdigitated geometry of the detection unit (a). Schematic circuit diagram of the prototype array (b). Picture of the prototype array with the housing (c).

2.2 Experimental set-up

The experiment was carried out at the PALS (Prague Asterix Laser System) facility of the Institute of Plasma Physics of the Czech Academy of Science (IPP- CAS) in Prague (CZ) using the Asterix Laser System operating at the fundamental wavelength of 1315 nm and delivering an average energy of 600 J in a pulse duration of 300 ps (FWHM) on target [27]. The laser beam was focused onto the target with a spot diameter of 80 µm and the laser intensity on target was $\sim 10^{16}$ W/cm^2. To maximize the laser-plasma absorption, the laser incidence angle was 30°. The target used for the experiment consists of hydrogenated silicon wafer, 10 µm in thickness, that will be called "SiH" target. In more detail, the silicon wafer was firstly hydrogenated by means of an annealing thermal treatment for 3 hours in an H-environment and cut in small pieces. After the laser-target interaction, protons, silicon and carbon ions (originating from surface contaminations) would be generated and detected by diamond detectors. The diamond prototype was placed at 30° respect to the target normal direction and at a distance of 170.5 cm from the target.

2.3 Discrimination technique

The TOF signal generated in diamond detector results from the overlapping of the different ion contribution reaching the detector at certain time, depending on their kinetic energy. In the particular case of the p-^{11}B fusion reaction, the protons accelerated in the laser-target interaction and the produced alpha particles in the nuclear reaction, can reach the detector simultaneously if their energies follow the $E_\alpha/E_p = m_\alpha/m_p$ ratio. Alpha particles produced in p-^{11}B fusion reaction, have a peaked energy ~4 MeV and reach the detector placed at a certain distance at the same TOF values of protons having energies of 1 MeV. The use of layers placed in front of the detectors might help in the discrimination, but only if the cut-off is independently measured. Therefore, the use of different diamond detectors with different adsorbers in front of them is necessary. Indeed, the concept of the discrimination technique is to use TOF measurements from diamond detectors nominally identical but with specific material filters of different thicknesses. These filters are used by exploiting the different stopping powers and ranges of ions of different species and energies in order to have online discrimination of accelerated particles from the plasma. Here, aluminum

2023 JINST 18 C07008

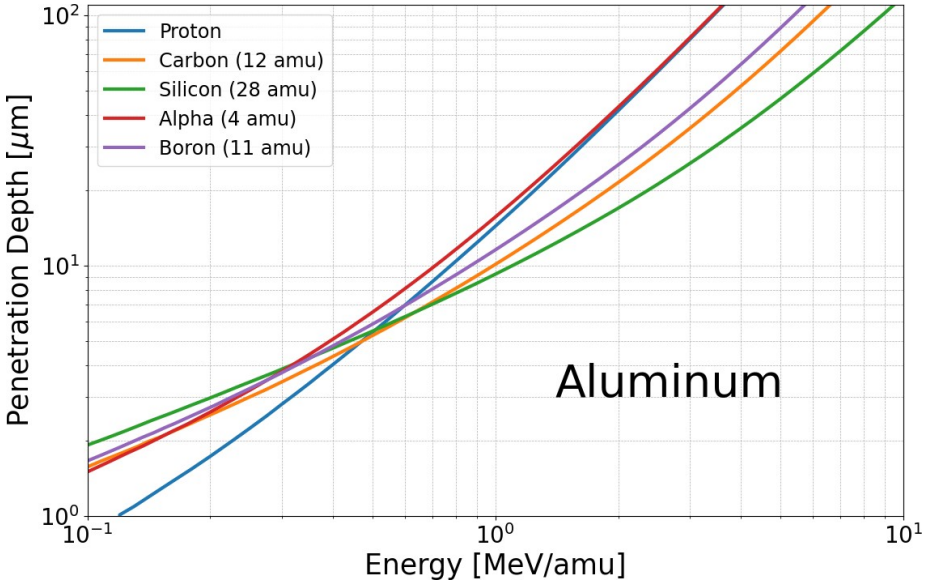

Figure 2. Penetration capacity in aluminum of ion species for a range of energy per nucleon from 100 keV to 10 MeV. Data obtained using SRIM software.

has been investigated through the Stopping and Range of Ions in Matter (SRIM) software [28], as shown in figure 2, where is reported the penetration depth of impinging ion species in aluminum as a function of energy per nucleon from 100 keV to 10 MeV. However, discrimination is not always possible. In fact, as can be seen from figure 2, it is clear that for low energy range it is difficult to distinguish between alpha, boron and carbon ions, while it is possible to discriminate protons and silicon ions. On the other hand, if we look at the energy range above ~2 MeV per nucleon, we see that it is not possible to discriminate protons from alpha ions but it is possible to discriminate other ions instead.

By the use of the Transport of Ions in Matter (TRIM) Monte Carlo computer program [28], a more rigorous approach was used to investigate four different energy values for protons and alpha to better understand their penetration depth spectra at fixed energy. The chosen energy values are related by the factor m_α/m_p ~4 and chosen in the region around 1 MeV for protons, this being the value from where a possible discrimination between protons and alpha starts to be challenging. Figure 3 shows the results of these simulations. In each simulation, 10^4 particles (per type) were generated and impinged on an aluminum layer with a orthogonal path to the surface and built histograms of the occurrences of the penetration depth at fixed particle energy. As it can be seen, spectra of 500 keV (figure 3a) and 750 keV (figure 3b) protons appear well separated from spectra of respectively 2 MeV and 3 MeV alpha particles. So using an appropriate thickness of aluminum would allow a clear discrimination between the two species during detection. For 1 MeV protons (figure 3c) there is starting to be a more pronounced overlap of the spectra. Assuming a 15.5 µm aluminum filter is used, the contribution on total hits due to protons is about 5%. For 2 MeV protons (figure 3d), on the other hand, it is clear that the two spectra are increasingly overlapping. Thus, an efficient discrimination between the two species of particles is more problematic.

2023 JINST 18 C07008

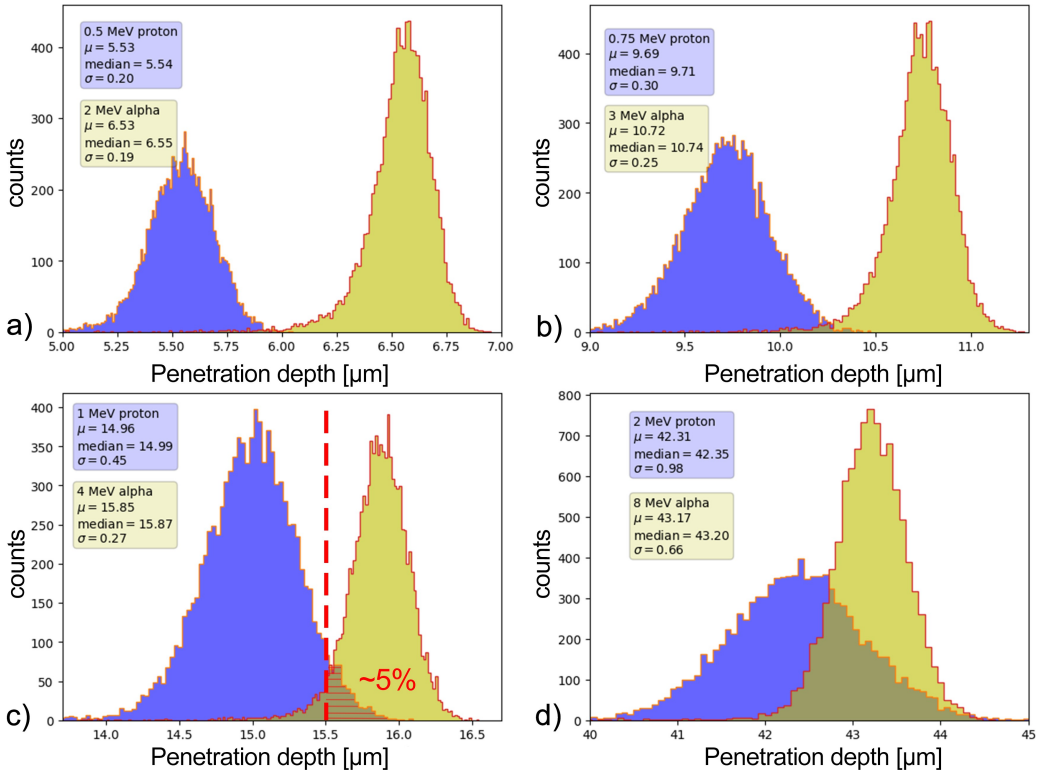

Figure 3. Histograms representing the penetration depth spectra of protons and alpha particles for several fixed energies on aluminum. Data obtained using TRIM program.

3 Results and discussions

To verify the uniform behavior of the four detectors, some shots were obtained in the naked configuration, i.e. without any kind of aluminum layer. The results of one of these shots have been shown in figure 4 (left). As it can be seen, the four diamond detectors, nominally identical, return very similar and overlapping TOF signals. The TOF signal shows the time evolution of particles reaching the detector after being emitted from the irradiated target. When the laser hits the surface of the target, UV and X-rays are also generated. They cause the initial photo-peak clearly visible at few ns, used as "starting time" of TOF technique. This is immediately followed by a tail typically generated by low energy electrons. In contrast, the second part of the TOF signal is due to a combination of fast protons, (peak around 100 ns), and heavier and slower ions (tail from 150 to 400 ns). The maximum proton energy was estimated to be around 2 MeV. The signal-to-noise ratio was not optimized for the developed prototype. A dedicated device housing could certainly improve the signal-to-noise ratio, giving better shielding the intense Electromagnetic Pulse (EMP) noise presents in the experiment [29]. After verifying the uniformity of detection responsivity of the four detectors in the array, three aluminum layers of different thicknesses, i.e. 10 µm, 15 µm and 20 µm, were placed respectively in front of D_{12}, D_{22}, D_{21} and data taking was started with this setup. An output of the four signals is shown in figure 4 (right). As expected, the signals from the three filtered detectors show significant attenuation, especially for photopeak and the tail due to the slow ions.

2023 JINST 18 C07008

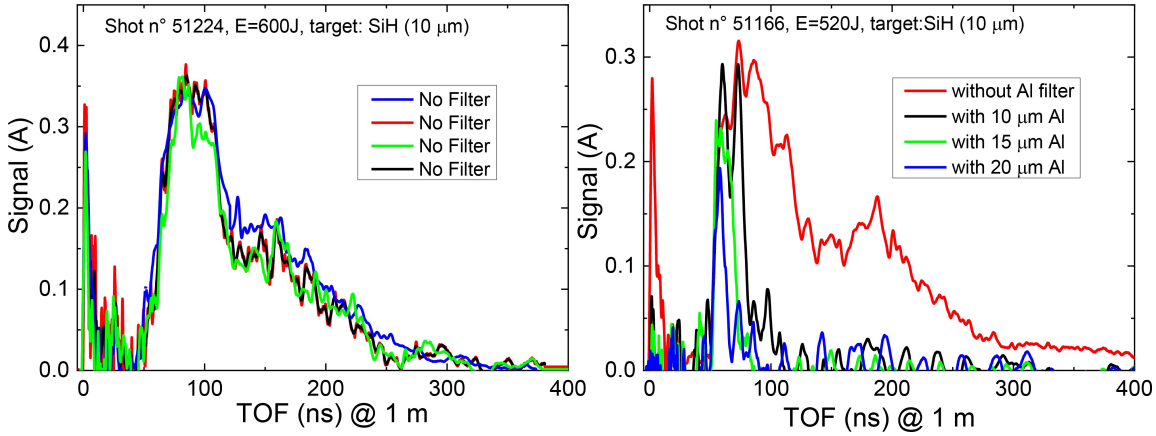

Figure 4. TOF signals output from the prototype array in the configuration without filters (left). TOF signals output from the prototype array in the configuration with aluminum filters (right).

From the data set obtained with the filtered configuration, the corresponding energy spectrum was derived by converting times values to energies, i.e. $\frac{1}{2}m_i\left(\frac{L}{\mathrm{TOF}}\right)^2$, where L is target-detector distance. Energy values are normalized by the m_i in order to have energy per nucleon values. From the energy spectrum measured by D_{11} (unfiltered detector) three discrepancy curves were derived by subtracting the spectra measured by D_{12}, D_{21} and D_{22}, as showed in figure 5 (left). Such spectra represent the energies lost in the three aluminum filters by the impinging ions from which is possible to estimate the cut-off energies. Plotting them against the nominally thickness of aluminum used, is reasonable to compare these points with the plots obtained with SRIM software of the energy of the ions against their penetration depth in the same material used for the layers. The maximum and minimum energy errors for each experimental point are evaluated from the corresponding 20% and 80% of signal in the cut-off range (see figure 5 (left)). This demonstrates how a fast detector benefits in terms of energy resolution. As it can be seen from figure 5 (right), the three points

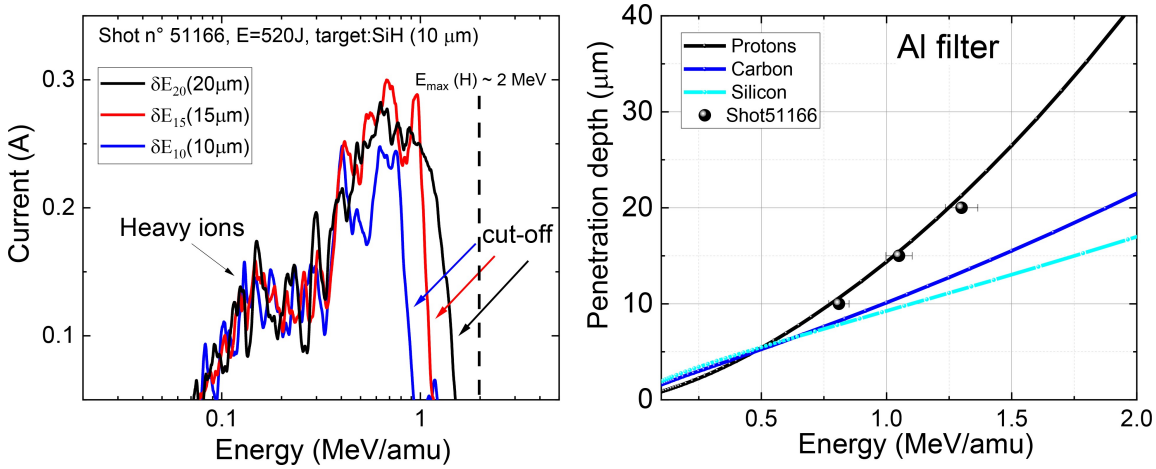

Figure 5. Discrepancy curves between the unfiltered detector and the three filtered detectors signals (left). Points representing the energy values corresponding to cut-off of the discrepancy curves plotted on the SRIM software-generated curves (right).

2023 JINST 18 C07008

appear to superimpose quite well on the curve expected for protons. This indicates that the ions generated by the plasma and accelerated toward the detector are mainly protons and not Si or C ions, which are both present in the target used in the experiment. This is surely true from energy above 0.75 MeV/amu. Indeed, at low energy range, a beveled peak due to contribution of heavy ions is clearly visible around 0.15 MeV/amu.

This preliminarily analysis is meant to serve as preparation for a more complete future experiment with rigorous and more satisfying data analysis. Indeed, the methodology reported in this work will be used for the discrimination of alpha particles from other ions in the framework of laser-driven p-^{11}B nuclear fusion experiments.

4 Conclusions

An array detector prototype composed of four single-crystal CVD diamond detectors with an interdigitated metal electrode, fabricated at the University of Rome "Tor Vergata", was used to carry on the study of the TOF technique for the diagnostics of laser-matter interaction products obtained at the PALS facility in Prague with a laser pulse of an intensity of about 10^{16} W/cm^2. In this work aluminum was used as element to discriminate accelerated particles by their energy lost in it. However, it is planned to study the same technique using other materials, not necessarily metals, to increase the discretizing capacity of this system. In addition, increasing the number of detectors in the array will increase the detector density and thus its efficiency and accuracy. Improving the housing of the prototype detector array with better materials and design will enhance shielding from the EMP, well present in plasma experiments. The preliminary results obtained in this work from a first use of the prototype array detector appear useful for future works in further development of this TOF technique for the purpose of discriminating different species of accelerated ions and the products diagnostics of the promising p-^{11}B reaction.

Acknowledgments

This work is supported by PALS (project number PALS002674) "New frontiers of nuclear reactions induced by laser-matter interaction: understanding and enhancing alpha-particle energy and yield in proton-boron fusion" financed by LaserLAB Europe and partially supported by INFN-FUSION Experiment. L. Giuffrida was supported by the project Advanced research using high intensity laser produced photons and particles (ADONIS) CZ.02.1.01/0.0/0.0/16_019/0000789 from European Regional Development Fund (ERDF) and from the European Union's Horizon 2020 research and innovation programme under grant agreement No. 871161. J.D. and M.K. greatly appreciate a financial support (grant no. LM2023068) from the Czech Ministry of Education, Youth and Sports making possible to operate the PALS facility. The authors thank the PALS facility staff for their technical support.

2023 JINST 18 C07008

References

[1] H. Daido, M. Nishiuchi and A.S. Pirozhkov, *Review of laser-driven ion sources and their applications*, *Rept. Prog. Phys.* **75** (2012) 056401.

[2] A. Macchi, *A Superintense Laser-Plasma Interaction Theory Primer*, Springer (2013) [DOI:10.1007/978-94-007-6125-4].

[3] M. Barberio, S. Veltri, M. Scisciò and P. Antici, *Laser-Accelerated Proton Beams as Diagnostics for Cultural Heritage*, *Sci. Rep.* **7** (2017) 40415.

[4] D. Doria et al., *Biological effectiveness on live cells of laser driven protons at dose rates exceeding* 10^9 *Gy/s*, *AIP Adv.* **2** (2012) 011209.

[5] S. Atzeni and J. Meyer-ter-Vehn, *The Physics of Inertial Fusion, Beam Plasma Interaction, Hydrodynamics, Hot Dense Matter*, Oxford University Press (2004) [DOI:10.1093/acprof:oso/9780198562641.001.0001].

[6] D.C. Moreau, *Potentiality of the proton-boron fuel for controlled thermonuclear fusion*, *Nucl. Fusion* **17** (1977) 13.

[7] W.M. Nevins and R. Swain, *The thermonuclear fusion rate coefficient for p-*^{11}B *reactions*, *Nucl. Fusion* **40** (2000) 865.

[8] V.F. Dmitriev, *α-particle spectrum in the reaction* $p + {}^{11}B \rightarrow \alpha + {}^{8}Be^{*} \rightarrow 3\alpha$, *Phys. Atom. Nucl.* **72** (2009) 1165.

[9] S. Stave et al., *Understanding the* $^{11}B(p,\alpha)\alpha\alpha$ *reaction at the* 0.675 *MeV resonance*, *Phys. Lett. B* **696** (2011) 26.

[10] D. Margarone et al., *In-target proton-boron nuclear fusion using a PW-class laser*, *Appl. Sci.* **12** (2022) 1444.

[11] D.-K. Yoon, J.-Y. Jung and T.S. Suh, *Application of proton boron fusion reaction to radiation therapy: A Monte Carlo simulation study*, *Appl. Phys. Lett.* **105** (2014) 223507.

[12] L. Giuffrida et al., *Prompt gamma ray diagnostics and enhanced hadron-therapy using neutron-free nuclear reactions*, *AIP Adv.* **6** (2016) 105204 [arXiv:1608.06778].

[13] F.P. Cammarata et al., *Proton boron capture therapy (PBCT) induces cell death and mitophagy in a heterotopic glioblastoma model*, *Commun. Biol.* **6** (2023) 388.

[14] G. Petringa et al., *Prompt gamma-ray emission for future imaging applications in proton-boron fusion therapy*, 2017 *JINST* **12** C03059.

[15] G. Petringa et al., *Study of gamma-ray emission by proton beam interaction with injected Boron atoms for future medical imaging applications*, 2017 *JINST* **12** C03049.

[16] S.M. Qaim et al., *Uses of alpha particles, especially in nuclear reaction studies and medical radionuclide production*, *Radiochim. Acta* **104** (2016) 601.

[17] K. Szkliniarz et al., *Production of medical Sc radioisotopes with an alpha particle beam*, *Appl. Radiat. Isot.* **118** (2016) 182.

[18] A. Picciotto et al., *Boron-Proton Nuclear-Fusion Enhancement Induced in Boron-Doped Silicon Targets by Low-Contrast Pulsed Laser*, *Phys. Rev. X* **4** (2014) 031030.

[19] C. Labaune et al., *Laser-initiated primary and secondary nuclear reactions in Boron-Nitride*, *Sci. Rep.* **6** (2016) 21202.

2023 JINST 18 C07008

[20] L. Giuffrida et al., *High-current stream of energetic α particles from laser-driven proton-boron fusion*, *Phys. Rev. E* **101** (2020) 013204.

[21] F. Consoli et al., *Diagnostic Methodologies of Laser-Initiated* $^{11}B(p,\alpha)2\alpha$ *Fusion Reactions*, *Front. Phys.* **8** (2020) 561492.

[22] J.E. Field, *Properties of Diamond*, Academic Press (1979).

[23] D. Kania, M. Landstrass, M. Plano, L. Pan and S. Han, *Diamond radiation detectors*, *Diam. Relat. Mater.* **2** (1993) 1012.

[24] V. Kantarelou et al., *A Methodology for the Discrimination of Alpha Particles from Other Ions in Laser-Driven Proton-Boron Reactions Using CR-39 Detectors Coupled in a Thomson Parabola Spectrometer*, *Laser Part. Beams* **2023** (2023) 1.

[25] C. Verona et al., *Comparison of single crystal diamond TOF detectors in planar and transverse configuration*, 2020 *JINST* **15** C09066.

[26] M. Salvadori et al., *Accurate spectra for high energy ions by advanced time-of-flight diamond-detector schemes in experiments with high energy and intensity lasers*, *Sci. Rep.* **11** (2021) 3071 [arXiv:2003.01442].

[27] K. Jungwirth et al., *The Prague Asterix Laser System*, *Phys. Plasmas* **8** (2001) 2495.

[28] http://www.srim.org/.

[29] F. Consoli et al., *Laser produced electromagnetic pulses: generation, detection and mitigation*, *High Power Laser Sci. Eng.* **8** (2020) e22.

2023 JINST 18 C07008